

RESEARCH ARTICLE

[View Article Online](#)
[View Journal](#) | [View Issue](#)



Cite this: *Org. Chem. Front.*, 2021, **8**, 3675

Received 23rd March 2021,
Accepted 4th May 2021
DOI: 10.1039/d1qo00457c
rsc.li/frontiers-organic

Pillar[5]arene-based ion-pair recognition for constructing a [2]pseudorotaxane with supramolecular interaction induced LCST behavior†

Ming Li, ^a Bin Hua ^{a,b} and Feihe Huang ^{a,b,c}

A LCST-type [2]pseudorotaxane based on perbromoethylated pillar[5]arene/imidazolium iodide ionic liquid ion-pair recognition is constructed in both solution and the solid state. The thermo-responsive behavior can be adjusted by altering the molar ratio of the host and guest as well as the concentrations of these two components in solution.

Introduction

Along with the advent and burgeoning of supramolecular chemistry, mechanically interlocked molecules (MIMs),^{1–5} due to their sophisticated topological architectures and potential applications in artificial molecular machines, have attracted significant interest in the scientific community.^{6–9} Various types of MIMs, such as rotaxanes, pseudorotaxanes and catenanes, have been widely used as smart building blocks for the creation of supramolecular systems and advanced functional materials.^{10–15} Pseudorotaxanes, which are supramolecular complexes but not compounds, can be considered as not only crucial fundamental precursors for the synthesis of rotaxanes and catenanes but also the prototypes of simple supramolecular chemical topologies and molecular devices.^{16–19} Considering the particular molecular architectures with fascinating properties and extensive applications of pseudorotaxanes, the design and preparation of novel pseudorotaxanes with the ability to perform functions are valuable and highly desirable for chemists.^{20–24}

Endowing pseudorotaxanes with strong binding ability is also highly important in constructing pseudorotaxanes. Ion-pair recognition, emerging from the coordination chemistry of cations and anions, has been proved to be an efficient strategy to construct robust pseudorotaxanes.²⁵ Typical ion-pair receptors contain disparate binding sites for complexing concurrently both cations and anions.²⁶ In particular, ion-pair recognition is believed to offer advantages in terms of strong affinity and selectivity during the recognition process, thus enhancing the binding strength and raising the association constants of the host–guest inclusion assemblies.^{27–30} Due to the affirmative cooperative effects, ion-pair recognition-based pseudorotaxanes have been widely utilized in diverse areas such as ion extraction, self-assembly and logic gate design.^{31–33} Therefore, exploring new systems for ion-pair recognition-based pseudorotaxanes with new properties and functionalities is still of great interest and importance, and will undoubtedly enrich the fundamental research and practical applications of ion-pair recognition chemistry.

Pillararenes, with unique symmetrical and rigid molecular architectures, have received significant attention and have experienced an extraordinary development in recent years.^{34–40} Due to abundant host–guest recognition properties, pillar[*n*]arenes and their derivatives have been proven to serve as ideal hosts for the fabrication of various MIMs and more advanced supramolecular structures.^{41–48} Herein, a new [2]pseudorotaxane based on perbromoethylated pillar[5]arene (**BrP5**) and 1,3-dimethylimidazolium iodide ionic liquid (**G1**) ion-pair recognition was successfully constructed (Scheme 1). Due to the introduction of ion-pair recognition, the binding ability of **BrP5**–**G1** was stronger than those of pseudorotaxanes formed between **BrP5** and other imidazolium-based ionic liquids with larger counterions. The hydrogen bonds between the hydrogen atoms on the bromoethyl chains of **BrP5** and the

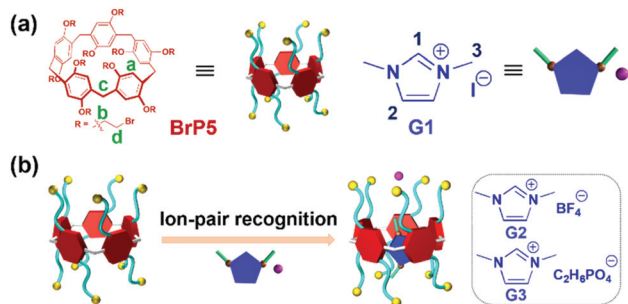
^aState Key Laboratory of Chemical Engineering, Key Laboratory of Excited-State Materials of Zhejiang Province, Stoddart Institute of Molecular Science, Department of Chemistry, Zhejiang University, Hangzhou 310027, China.

E-mail: huabin@zju.edu.cn; fhuang@zju.edu.cn; Fax: +86-571-8795-3189; Tel: +86-571-8795-3189

^bZJU-Hangzhou Global Scientific and Technological Innovation Center, Hangzhou, 311215, China

^cGreen Catalysis Center and College of Chemistry, Zhengzhou University, Zhengzhou 450001, China

† Electronic supplementary information (ESI) available: X-ray crystallographic files (CIF), experimental details, NMR spectra and other materials (PDF). CCDC 2065029. For ESI and crystallographic data in CIF or other electronic format see DOI: 10.1039/d1qo00457c



Scheme 1 (a) Chemical structures and cartoon representations of **BrP5** and **G1** used in this study. (b) Schematic representation of the ion-pair recognition process of **BrP5** and **G1** to form a [2]pseudorotaxane and chemical structures of **G2** and **G3** with different counterions.

iodide anions of **G1** have greatly contributed to the formation of such a [2]pseudorotaxane. Interestingly, the [2]pseudorotaxane **BrP5**–**G1** showed lower critical solution temperature (LCST) phase transition behaviors which can be modulated by altering the molar ratio of the host and guest as well as the concentrations of these two components in solution.

Results and discussion

Initially, to investigate the complexation behavior of **BrP5** and **G1**, ^1H NMR spectroscopy was conducted as a useful method to study the host–guest interactions. Significant chemical shift changes of the proton signals on both **BrP5** and **G1** occurred upon mixing them in CDCl_3 . Obviously, as shown in Fig. 1, all the peaks related to protons H_2 and H_3 on **G1** displayed conspicuous upfield shifts and remarkable complexation-induced broadening effects compared with those of free **G1**. Moreover, the proton signal of H_1 on **G1** could not be observed after the formation of the host–guest complex, indicating that the imidazolium part of **G1** was fully located in the cavity of **BrP5** and

shielded by the electron-rich cyclic structure (ESI, Fig. S2†). Besides, the peaks of protons H_a , H_b , H_c and H_d on **BrP5** also exhibited chemical shift changes due to the host–guest interactions. It could be speculated that the extensive changes of the chemical shifts and shapes of proton signals on **BrP5** and **G1** resulted from the formation of the inclusion complex, in which the guest protons were located within the cavity of **BrP5**. Then, 2D NOESY NMR spectroscopy was carried out to investigate the host–guest complex with an interpenetrated geometry. As shown in Fig. 2, nuclear Overhauser effect (NOE) correlations were observed between the signals related to proton H_2 on **G1** and protons H_b – H_d on **BrP5**, indicating that **G1** penetrated the cavity of **BrP5**.

Further proton NMR titration experiments (ESI, Fig. S3–S5†) were carried out to measure the complexation stoichiometry and association constant for the complexation between **BrP5** and **G1** in CDCl_3 . A 1:1 stoichiometry for the complexation was obtained from a mole ratio plot based on the chemical shift changes of H_a on **BrP5**. The association constant (K_a) was estimated to be $967 \pm 72 \text{ M}^{-1}$ in chloroform-*d* using the curve-fitting analysis method. The formation of the [2]pseudorotaxane was further confirmed by a low-resolution electrospray ionization mass spectrum (ESI-MS). The spectrum (ESI, Fig. S10†) showed a peak at m/z 1776.4, corresponding to $[\text{BrP5} \supset \text{G1} - \text{I}]^+$, which was in agreement with the result of the above-mentioned ^1H NMR experiments. All these phenomena provided strong evidence for the formation of a stable [2]pseudorotaxane in a 1:1 host-to-guest stoichiometry between **BrP5** and **G1** in solution.

To gain a deep insight into the [2]pseudorotaxane and its binding properties, single crystals suitable for X-ray diffraction analysis were obtained by slow diffusion of isopropyl ether into a solution of **BrP5** and **G1** in chloroform (ESI, Table S1†). The single crystal structure between the pillararene and the ionic liquid was obtained, providing direct evidence for their host–guest complexation behavior.^{49–51} As shown in Fig. 3, the

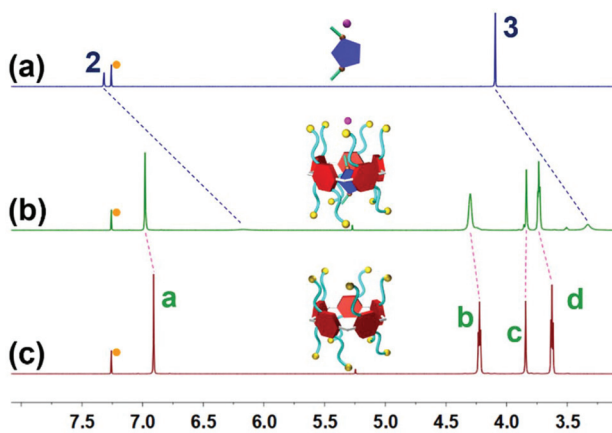


Fig. 1 Partial ^1H NMR spectra (600 MHz, CDCl_3 , room temperature): (a) **G1**; (b) **BrP5** (10.0 mM) and **G1** (10.0 mM); and (c) **BrP5**. The peaks marked with orange dots are ascribed to chloroform-*d*.

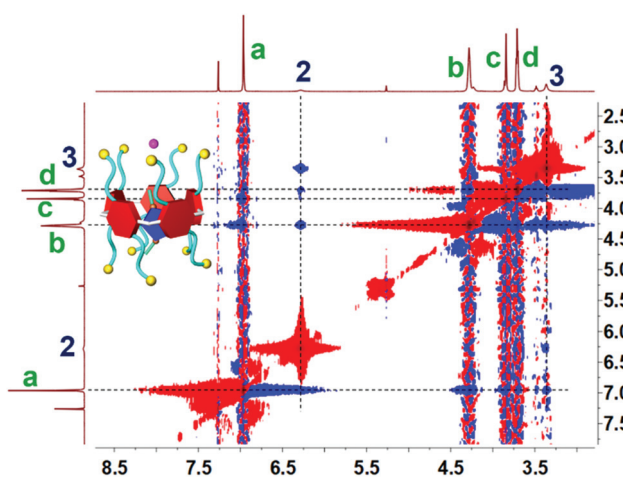


Fig. 2 Partial 2D ^1H – ^1H NOESY spectrum (500 MHz, CDCl_3 , room temperature) of the [2]pseudorotaxane **BrP5**–**G1**. $[\text{BrP5}] = 10.0 \text{ mM}$. $[\text{G1}] = 10.0 \text{ mM}$.

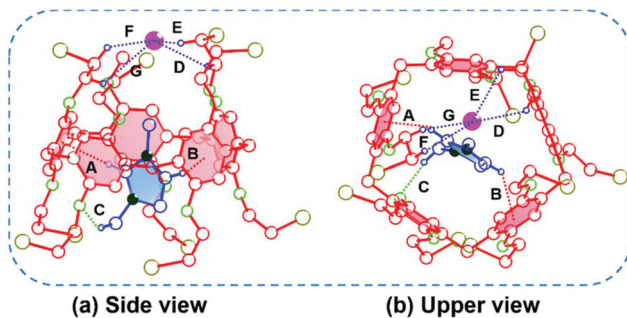


Fig. 3 Ball-stick views of the crystal structure of $\text{BrP5}\supset\text{G1}$: (a) side view and (b) upper view. Host BrP5 is red, guest G1 is blue, hydrogen atoms are blue, oxygen atoms are green, nitrogen atoms are solid and dark green, bromine atoms are dark yellow, and iodine atoms are solid and magenta. The red dashed lines indicate $\text{C}-\text{H}\cdots\pi$ interactions (A and B), the green dashed line indicates $\text{C}-\text{H}\cdots\text{O}$ interaction (C) and the blue dashed lines indicate $\text{C}-\text{H}\cdots\text{I}^-$ interactions (D, E, F and G). $\text{C}-\text{H}\cdots\pi$ interaction parameters are as follows: $\text{H}\cdots\pi$ -plane distances (angstroms) and $\text{C}-\text{H}\cdots\pi$ angles (degrees): A, 2.48, 152.28; B, 2.72, 141.30. $\text{C}-\text{H}\cdots\text{O}$ interaction parameters: $\text{C}-\text{H}\cdots\text{O}$ distance (angstrom) and $\text{C}-\text{H}\cdots\text{O}$ angle (degree): C, 2.60, 139.21. $\text{C}-\text{H}\cdots\text{I}^-$ interaction parameters: $\text{C}-\text{H}\cdots\text{I}^-$ distances (angstroms): D, 2.98; E, 2.98; F, 2.71; and G, 3.14. $\text{C}-\text{H}\cdots\text{I}^-$ angles (degrees): D, 126.45; E, 112.06; F, 134.56; and G, 116.83. Hydrogen atoms that do not have interactions with other atoms are removed for clarity.

[2]pseudorotaxane was indeed formed with the imidazolium part of G1 located in the central cavity of the host BrP5 , which was in accordance with the NMR experimental results in solution. In this crystal structure, the imidazolium part inside the cavity established a couple of $\text{C}-\text{H}\cdots\pi$ interactions (A and B) with the benzene rings of BrP5 with $\text{H}\cdots\pi$ plane distances of 2.48 Å and 2.72 Å and $\text{C}-\text{H}\cdots\pi$ angles of 152.28° and 141.30°, respectively. Furthermore, a $\text{C}-\text{H}\cdots\text{O}$ interaction (C) was also observed between a hydrogen atom on G1 and an oxygen atom on BrP5 with a $\text{C}-\text{H}\cdots\text{O}$ distance of 2.60 Å and an angle of 139.21°. These interactions were believed to contribute to the stability of this [2]pseudorotaxane. Another essential contribution to the formation of these structures was that the iodide anion was captured in the cavity of BrP5 , mainly stabilized by four $\text{C}-\text{H}\cdots\text{I}^-$ interactions (D, E, F and G). The distances between the iodide anion and bromoethoxy hydrogen atoms of BrP5 were calculated to be 2.98, 2.98, 2.71 and 3.14 Å, respectively, which were smaller than the sum of the van der Waals radii of the iodide anion and the hydrogen atom (3.40 Å), suggesting the presence of $\text{C}-\text{H}\cdots\text{I}^-$ interactions.^{52,53}

Besides, it should be noted that the binding affinity of the [2]pseudorotaxane $\text{BrP5}\supset\text{G1}$ was promoted and enhanced by the ion-pair recognition, and different counterions of the imidazolium-based ionic liquid have a huge influence on the association behavior. To prove this, imidazolium guests G2 with a large tetrafluoroborate anion and G3 with a dimethylphosphate anion were used as guests to investigate the binding properties of BrP5 . The association constant K_a between G2 and BrP5 was determined to be $89 \pm 20 \text{ M}^{-1}$ in chloroform-*d*, which was smaller than that of $\text{BrP5}\supset\text{G1}$ (ESI),

Fig. S6–S8†). Besides, in the titration process of a solution of G3 with a larger dimethylphosphate anion into BrP5 , no significant shifts for the host protons H_a were observed even after the addition of 6.0 equiv. of G3 (ESI, Fig. S9†). This observation implies very weak complexation between BrP5 and G3 . Accordingly, the association constant could not be calculated for this complex. These results indicated that the counterions on the guests played significant roles in the host–guest association process, and demonstrated that the ion-pair recognition showed a positive effect during molecular recognition.

Intriguingly, after the establishment of the ion-pair recognition motif between BrP5 and G1 , the [2]pseudorotaxane showed supramolecular interaction-induced LCST phase behavior. Next, we aimed to investigate its functionality in LCST behavior. Firstly, due to the relatively poor solubility of the ionic liquid G1 in chloroform at room temperature, an immiscible solution was obtained by mixing a relatively high concentration of G1 with chloroform. In Fig. 4a, we can see that the mixture transformed from two separated phases into one transparent solution after adding BrP5 to establish the host–guest complexation with G1 . The possible reason is that the host–guest complex has better solubility in chloroform. Notably, the solution exhibited a significant thermoresponsive behavior. The clear solution became opaque on heating and then turned back to transparent again upon cooling (Fig. 4a). The course of change was fully reversible. The explanation of

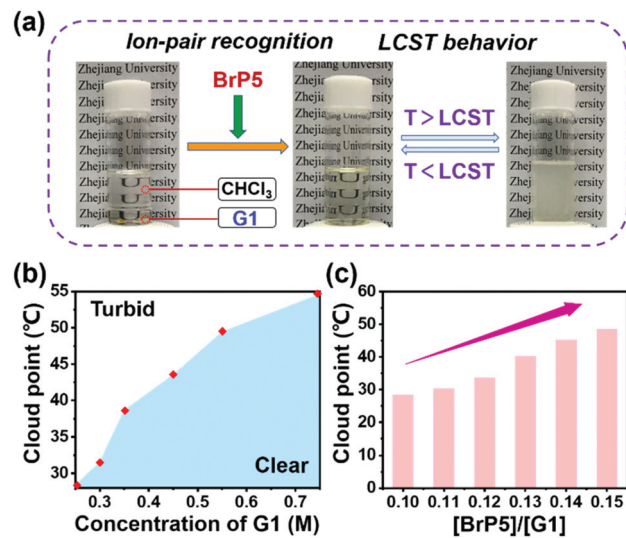


Fig. 4 (a) Illustration of host–guest ion-pair recognition and supramolecular interaction induced LCST behavior of the [2]pseudorotaxane $\text{BrP5}\supset\text{G1}$: the transparent solution was formed after the addition of BrP5 into the two immiscible phases of G1 and chloroform and its LCST-type phase changes. (b) Concentration dependence of the cloud point of G1 in the presence of BrP5 in chloroform. The initial concentrations of G1 were 0.25 M, 0.30 M, 0.35 M, 0.45 M, 0.55 M and 0.75 M, from left to right, respectively, and the molar ratio of BrP5 to G1 was kept constant at 0.10. (c) Change of the cloud point upon altering the molar ratio of BrP5 to G1 (0.10, 0.11, 0.12, 0.13, 0.14 and 0.15, from left to right, respectively, while the concentration of G1 was maintained at 0.25 M).

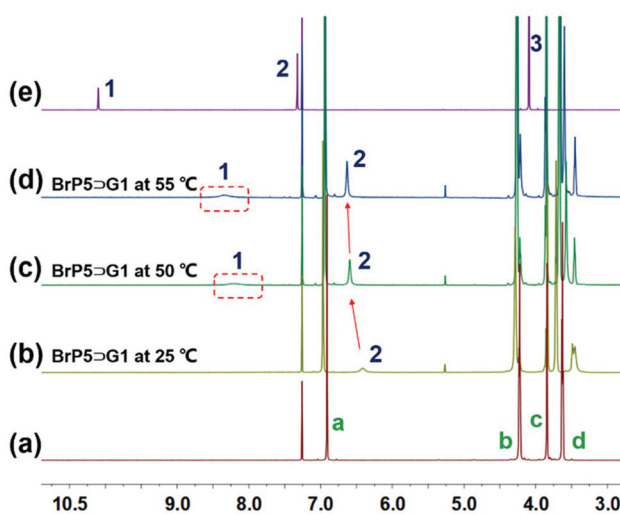


Fig. 5 Partial temperature-dependent ^1H NMR spectra (600 MHz, CDCl_3): (a) BrP5 at 25 °C; (b) $\text{BrP5}\supset\text{G1}$ at 25 °C; (c) $\text{BrP5}\supset\text{G1}$ at 50 °C; (d) $\text{BrP5}\supset\text{G1}$ at 55 °C; and (e) G1 at 25 °C.

such a tunable LCST behavior was ascribed to the fact that the complexation affinity between **BrP5** and **G1** in the [2]pseudorotaxane was temperature dependent. When the temperature increased, the interactions between **BrP5** and **G1** were weakened or even destroyed, and the disassembly of the [2]pseudorotaxane resulted in the release of **G1** from the cyclic cavity of **BrP5** to the chloroform solution. Temperature-variable ^1H NMR experiments (Fig. 5) showed that as the temperature increased, changes occurred in the chemical shifts related to the protons on both **BrP5** and **G1**. In particular, the signals of protons H_1 on **G1** of the [2]pseudorotaxane gradually appeared, which were completely shielded by the cyclic structure before.

The concentration-dependent characteristic of the complexation-induced LCST behavior was investigated next. As the concentration of **G1** increased from 0.25 M to 0.75 M (the molar ratio of **BrP5** to **G1** was kept constant at 0.10), the cloud point (T_{cloud}) gradually increased from 28.4 to 54.6 °C (Fig. 4b and ESI, Fig. S11a†). Furthermore, the system also showed molar ratio-dependent behavior (Fig. 4c and ESI, Fig. S11b†). While we fixed the concentration of **G1** at 0.25 M, upon altering the molar ratio of **BrP5** to **G1** from 0.10 to 0.15, the T_{cloud} changed accordingly from 28.4 to 48.4 °C. Besides, DLS results revealed that the size of the nanostructure of this LCST system changed immensely at different temperatures. For example, a system with the T_{cloud} found to be around 28.4 °C by monitoring the transmittance change showed average sizes of 7.87 ± 0.89 nm and 703 ± 85.1 nm below and above the LCST, respectively (ESI, Fig. S12†).

Conclusions

In summary, we developed a novel [2]pseudorotaxane based on perbromoethylated pillar[5]arene/imidazolium iodide ionic

liquid ion-pair recognition in both solution and the solid state. The introduction of ion-pair recognition contributed greatly to the stability of the [2]pseudorotaxane. In addition, experimental results demonstrated that the thermosensitive phase behavior of the [2]pseudorotaxane can be affected by the molar ratio of the host to guest at a certain concentration or the concentrations of these two components at a certain molar ratio. This work not only enriched pillararene-based threaded structures but also constructed a smart functional supramolecular material. The exploration of such interesting pseudorotaxanes with extra functions will provide some helpful hints for the design of more advanced functional materials such as molecular sensors^{54,55} and stimuli-responsive functional supramolecular systems.

Conflicts of interest

There are no conflicts to declare.

Acknowledgements

This work was supported by the National Natural Science Foundation of China (22035006) and the Zhejiang Provincial Natural Science Foundation of China (LD21B020001).

Notes and references

- 1 A. C. Fahrenbach, C. J. Bruns, H. Li, A. Trabolsi, A. Coskun and J. F. Stoddart, Ground-State Kinetics of Bistable Redox-Active Donor-Acceptor Mechanically Interlocked Molecules, *Acc. Chem. Res.*, 2014, **47**, 482–493.
- 2 K. Kim, Mechanically Interlocked Molecules Incorporating Cucurbituril and Their Supramolecular Assemblies, *Chem. Soc. Rev.*, 2002, **31**, 96–107.
- 3 S. Mena-Hernando and E. M. Pérez, Mechanically Interlocked Materials. Rotaxanes and Catenanes Beyond the Small Molecule, *Chem. Soc. Rev.*, 2019, **48**, 5016–5032.
- 4 J. F. Stoddart, Mechanically Interlocked Molecules (MIMs) —Molecular Shuttles, Switches, and Machines (Nobel Lecture), *Angew. Chem., Int. Ed.*, 2017, **56**, 11094–11125.
- 5 W.-J. Li, W. Wang, X.-Q. Wang, M. Li, Y. Ke, R. Yao, J. Wen, G.-Q. Yin, B. Jiang, X. Li, P. Yin and H.-B. Yang, Daisy Chain Dendrimers: Integrated Mechanically Interlocked Molecules with Stimuli-Induced Dimension Modulation Feature, *J. Am. Chem. Soc.*, 2020, **142**, 8473–8482.
- 6 C. Pezzato, C. Cheng, J. F. Stoddart and R. D. Astumian, Mastering the Non-Equilibrium Assembly and Operation of Molecular Machines, *Chem. Soc. Rev.*, 2017, **46**, 5491–5507.
- 7 Y.-L. Zhao, H.-Y. Zhang, D.-S. Guo and Y. Liu, Nanoarchitectures Constructed from Resulting Polypseudorotaxanes of the β -Cyclodextrin/4,4'-Dipyridine Inclusion Complex with Co^{2+} and Zn^{2+} Coordination Centers, *Chem. Mater.*, 2006, **18**, 4423–4429.

8 X. Ge, Y. He, X. Liang, L. Wu, Y. Zhu, Z. Yang, M. Hu and T. Xu, Thermally Triggered Polyrotaxane Translational Motion Helps Proton Transfer, *Nat. Commun.*, 2018, **9**, 2297.

9 H. Li, X. Li, H. Ågren and D.-H. Qu, Two Switchable Star-Shaped [1](*n*)Rotaxanes with Different Multibranched Cores, *Org. Lett.*, 2014, **16**, 4940–4943.

10 L. Wang, L. Cheng, G. Li, K. Liu, Z. Zhang, P. Li, S. Dong, W. Yu, F. Huang and X. Yan, A Self-Cross-Linking Supramolecular Polymer Network Enabled by Crown-Ether-Based Molecular Recognition, *J. Am. Chem. Soc.*, 2020, **142**, 2051–2058.

11 G. Li, L. Wang, L. Wu, Z. Guo, J. Zhao, Y. Liu, R. Bai and X. Yan, Woven Polymer Networks via the Topological Transformation of a [2]Catenane, *J. Am. Chem. Soc.*, 2020, **142**, 14343–14349.

12 X.-K. Ma, Y.-M. Zhang, Q. Yu, H. Zhang, Z. Zhang and Y. Liu, A Twin-Axial Pseudorotaxane for Phosphorescence Cell Imaging, *Chem. Commun.*, 2021, **57**, 1214–1217.

13 M. Liu, S. Li, M. Zhang, Q. Zhou, F. Wang, M. Hu, F. R. Fronczeck, N. Li and F. Huang, Three-Dimensional Bis(m-phenylene)-32-Crown-10-Based Cryptand/Paraquat Catenanes, *Org. Biomol. Chem.*, 2009, **7**, 1288–1291.

14 M. Zhang, X. Yan, F. Huang, Z. Niu and H. W. Gibson, Stimuli-Responsive Host–Guest Systems Based on the Recognition of Cryptands by Organic Guests, *Acc. Chem. Res.*, 2014, **47**, 1995–2005.

15 M. Zhang, L. Cao and L. Isaacs, Cucurbit[6]uril–Cucurbit[7]uril Heterodimer Promotes Controlled Self-Assembly of Supramolecular Networks and Supramolecular Micelles by Self-Sorting of Amphiphilic Guests, *Chem. Commun.*, 2014, **50**, 14756–14759.

16 X. Wu, Y. Yu, L. Gao, X.-Y. Hu and L. Wang, Stimuli-Responsive Supramolecular Gel Constructed by Pillar[5]arene-Based Pseudo[2]rotaxanes via Orthogonal Metal-Ligand Coordination and Hydrogen Bonding Interaction, *Org. Chem. Front.*, 2016, **3**, 966–970.

17 X. Ma, Q. Wang, D. Qu, Y. Xu, F. Ji and H. Tian, A Light-Driven Pseudo[4]rotaxane Encoded by Induced Circular Dichroism in a Hydrogel, *Adv. Funct. Mater.*, 2007, **17**, 829–837.

18 C. Biagini, S. D. P. Fielden, D. A. Leigh, F. Schaufelberger, S. Di Stefano and D. Thomas, Dissipative Catalysis with a Molecular Machine, *Angew. Chem.*, 2019, **58**, 9876–9880.

19 G. De Bo, M. A. Y. Gall, M. O. Kitching, S. Kuschel, D. A. Leigh, D. J. Tetlow and J. W. Ward, Sequence-Specific β -Peptide Synthesis by a Rotaxane-Based Molecular Machine, *J. Am. Chem. Soc.*, 2017, **139**, 10875–10879.

20 A. K. Mandal, M. Gangopadhyay and A. Das, Photo-Responsive Pseudorotaxanes and Assemblies, *Chem. Soc. Rev.*, 2015, **44**, 663–676.

21 Y.-M. Zhang, Y.-F. Li, H. Fang, J.-X. He, B.-R. Yong, H. Yao, T.-B. Wei and Q. Lin, Multi-Stimuli-Responsive Supramolecular Gel Constructed by Pillar[5]arene-Based Pseudorotaxanes for Efficient Detection and Separation of Multi-Analytes in Aqueous Solution, *Soft Matter*, 2018, **14**, 8529–8536.

22 X. Li, H.-S. Xu, K. Leng, S. W. Chee, X. Zhao, N. Jain, H. Xu, J. Qiao, Q. Gao, I.-H. Park, S. Y. Quek, U. Mirsaidov and K. P. Loh, Partitioning the Interlayer Space of Covalent Organic Frameworks by Embedding Pseudorotaxanes in Their Backbones, *Nat. Chem.*, 2020, **12**, 1115–1122.

23 M. Baroncini, S. Silvi and A. Credi, Photo- and Redox-Driven Artificial Molecular Motors, *Chem. Rev.*, 2020, **120**, 200–268.

24 H. Yin, Q. Huang, W. Zhao, D. Bardelang, D. Siri, X. Chen, S. M. Y. Lee and R. Wang, Supramolecular Encapsulation and Bioactivity Modulation of a Halonium Ion by Cucurbit[*n*]uril (*n*=7, 8), *J. Org. Chem.*, 2018, **83**, 4882–4887.

25 S. K. Kim and J. L. Sessler, Ion Pair Receptors, *Chem. Soc. Rev.*, 2010, **39**, 3784–3809.

26 P. A. Gale, Anion and Ion-pair Receptor Chemistry: Highlights from 2000 and 2001, *Coord. Chem. Rev.*, 2003, **240**, 191–221.

27 B. Hua, L. Shao, Z. Zhang, J. Liu and F. Huang, Cooperative Silver Ion-Pair Recognition by Peralkylated Pillar[5]arenes, *J. Am. Chem. Soc.*, 2019, **141**, 15008–15012.

28 L. Shao, B. Hua, J. Liu and F. Huang, Construction of a [2]Pseudorotaxane and a [3]Pseudorotaxane Based on Perbromoethylated Pillar[5]arene/Pyridinium Iodide Ion-Pair Recognition, *Chem. Commun.*, 2019, **55**, 4527–4530.

29 K. Zhu, S. Li, F. Wang and F. Huang, Anion-Controlled Ion-Pair Recognition of Paraquat by a Bis(m-phenylene)-32-crown-10 Derivative Heteroditopic Host, *J. Org. Chem.*, 2009, **74**, 1322–1328.

30 K. Zhu, M. Zhang, F. Wang, N. Li, S. Li and F. Huang, Improved Complexation between Dibenzo-24-crown-8 Derivatives and Dibenzylammonium Salts by Ion-Pair Recognition, *New J. Chem.*, 2008, **32**, 1827–1830.

31 S. K. Kim and J. L. Sessler, Calix[4]pyrrole-Based Ion Pair Receptors, *Acc. Chem. Res.*, 2014, **47**, 2525–2536.

32 A. J. McConnell and P. D. Beer, Heteroditopic Receptors for Ion-Pair Recognition, *Angew. Chem., Int. Ed.*, 2012, **51**, 5052–5061.

33 Q. He, Z. Zhang, J. T. Brewster, V. M. Lynch, S. K. Kim and J. L. Sessler, Hemispherand-Strapped Calix[4]pyrrole: An Ion-pair Receptor for the Recognition and Extraction of Lithium Nitrite, *J. Am. Chem. Soc.*, 2016, **138**, 9779–9782.

34 T. Ogoshi, T.-a. Yamagishi and Y. Nakamoto, Pillar-Shaped Macrocyclic Hosts Pillar[*n*]arenes: New Key Players for Supramolecular Chemistry, *Chem. Rev.*, 2016, **116**, 7937–8002.

35 J.-R. Wu, A. U. Mu, B. Li, C.-Y. Wang, L. Fang and Y.-W. Yang, Desymmetrized Leaning Pillar[6]arene, *Angew. Chem., Int. Ed.*, 2018, **57**, 9853–9858.

36 K. Velmurugan, M. Mohan, B. Li, K. Wang, M. Zuo and X.-Y. Hu, Macrocycles-Assisted Polymeric Self-Assemblies Fabricated by Host–Guest Complexation and Their Applications, *Mater. Adv.*, 2020, **1**, 2646–2662.

37 M. Li, B. Hua, H. Liang, J. Liu, L. Shao and F. Huang, Supramolecular Tessellations via Pillar[*n*]arenes-Based Exo-Wall Interactions, *J. Am. Chem. Soc.*, 2020, **142**, 20892–20901.

38 H. Zhang, Z. Liu and Y. Zhao, Pillararene-Based Self-Assembled Amphiphiles, *Chem. Soc. Rev.*, 2018, **47**, 5491–5528.

39 T. Kakuta, T.-a. Yamagishi and T. Ogoshi, Stimuli-Responsive Supramolecular Assemblies Constructed from Pillar[n]arenes, *Acc. Chem. Res.*, 2018, **51**, 1656–1666.

40 T. Xiao, L. Qi, W. Zhong, C. Lin, R. Wang and L. Wang, Stimuli-Responsive Nanocarriers Constructed from Pillar[n]arene-Based Supra-Amphiphiles, *Mater. Chem. Front.*, 2019, **3**, 1973–1993.

41 C. Li, K. Han, J. Li, H. Zhang, J. Ma, X. Shu, Z. Chen, L. Weng and X. Jia, Synthesis of Pillar[5]arene Dimers and Their Cooperative Binding toward Some Neutral Guests, *Org. Lett.*, 2012, **14**, 42–45.

42 X.-Y. Hu, P. Zhang, X. Wu, W. Xia, T. Xiao, J. Jiang, C. Lin and L. Wang, Pillar[5]arene-Based Supramolecular Polypseudorotaxanes Constructed from Quadruple Hydrogen Bonding, *Polym. Chem.*, 2012, **3**, 3060–3063.

43 S. Dong, B. Zheng, Y. Yao, C. Han, J. Yuan, M. Antonietti and F. Huang, LCST-Type Phase Behavior Induced by Pillar[5]arene/Ionic Liquid Host–Guest Complexation, *Adv. Mater.*, 2013, **25**, 6864–6867.

44 Q. Li, Y. Liu, P. Liu, L. Shangguan, H. Zhu and B. Shi, Solvent-controlled assembly of pillar[5]arene-based supramolecular networks via π – π interactions for white light modulation, *Org. Chem. Front.*, 2020, **7**, 399–404.

45 K. Jie, M. Liu, Y. Zhou, M. A. Little, S. Bonakala, S. Y. Chong, A. Stephenson, L. Chen, F. Huang and A. I. Cooper, Styrene Purification by Guest-Induced Restructuring of Pillar[6]arene, *J. Am. Chem. Soc.*, 2017, **139**, 2908–2911.

46 J.-R. Wu, B. Li and Y.-W. Yang, Separation of Bromoalkanes Isomers by Nonporous Adaptive Crystals of Leaning Pillar[6]arene, *Angew. Chem.*, 2020, **59**, 2251–2255.

47 X. Shu, W. Chen, D. Hou, Q. Meng, R. Zheng and C. Li, Novel Binding Regioselectivity in the Interpenetration of a Non-Symmetric Axe into a Non-Symmetric Pillar[5]arene Wheel, *Chem. Commun.*, 2014, **50**, 4820–4823.

48 T. Ogoshi, R. Sueto, M. Yagyu, R. Kojima, T. Kakuta, T.-a. Yamagishi, K. Doitomi, A. K. Tummanapelli, H. Hirao, Y. Sakata, S. Akine and M. Mizuno, Molecular Weight Fractionation by Confinement of Polymer in One-Dimensional Pillar[5]arene Channels, *Nat. Commun.*, 2019, **10**, 479.

49 C. Li, L. Zhao, J. Li, X. Ding, S. Chen, Q. Zhang, Y. Yu and X. Jia, Self-Assembly of [2]Pseudorotaxanes Based on Pillar[5]arene and Bis(imidazolium) Cations, *Chem. Commun.*, 2010, **46**, 9016–9018.

50 L. Gao, Y. Yao, S. Dong and J. Yuan, Host–Guest Complexation Between 1,4-Dipropoxypillar[5]arene and Imidazolium-Based Ionic Liquids, *RSC Adv.*, 2014, **4**, 35489–35492.

51 S. Dong, J. Yuan and F. Huang, A Pillar[5]arene/Imidazolium [2]Rotaxane: Solvent- and Thermo-Driven Molecular Motions and Supramolecular Gel Formation, *Chem. Sci.*, 2014, **5**, 247–252.

52 R. Shannon, Revised Effective Ionic Radii and Systematic Studies of Interatomic Distances in Halides and Chalcogenides, *Acta Crystallogr., Sect. A: Cryst. Phys., Diff., Theor. Gen. Crystallogr.*, 1976, **32**, 751–767.

53 A. Bondi, van der Waals Volumes and Radii, *J. Phys. Chem.*, 1964, **68**, 441–451.

54 S. Sun, J.-B. Shi, Y.-P. Dong, C. Lin, X.-Y. Hu and L.-Y. Wang, A Pillar[5]arene-Based Side-Chain Pseudorotaxanes and Polypseudorotaxanes as Novel Fluorescent Sensors for the Selective Detection of Halogen Ions, *Chin. Chem. Lett.*, 2013, **24**, 987–992.

55 O. Y. Kweon, S. K. Samanta, Y. Won, J. H. Yoo and J. H. Oh, Stretchable and Self-Healable Conductive Hydrogels for Wearable Multimodal Touch Sensors with Thermoresponsive Behavior, *ACS Appl. Mater. Interfaces*, 2019, **11**, 26134–26143.